

Influence of the presence of deuterium on displacement damage in tungsten

T. Schwarz Selinger¹, J. Bauer¹ und S. Markelj²

¹Max-Planck-Institut für Plasmaphysik, Boltzmannstr. 2, D-85748 Garching, Germany

²Institut Jožef Stefan, Jamova Cesta, 1000 Ljubljana, Slovenia

E-mail: schwarz-selinger@ipp.mpg.de

Abstract.

The influence of the presence of deuterium on displacement damage in tungsten is studied by implanting 20 MeV tungsten ions to a fluence equivalent to 0.23 dpa in the damage peak maximum into already displacement-damaged tungsten containing 1.7 at.% deuterium. SDTrimSP calculations reveal that for the tungsten implantation fluence used, on average each D atom is recoiled once and hence mobile deuterium should be present simultaneously while displacing tungsten atoms. Nuclear reaction analysis after the tungsten implantation shows that no deuterium is lost from the sample and the depth profile is unchanged. However, deuterium must have been de-trapped and is effectively re-trapped again because temperature programmed desorption spectroscopy (TPD) reveals that deuterium is redistributed from the low temperature de-trapping peak to the high temperature de-trapping peak. Rate equation modelling can describe the measured deuterium desorption with the same de-trapping energies as for the initial material but with increased trap densities only. Decorating the samples after the additional tungsten ion implantation again with a low energy deuterium plasma shows increased deuterium retention beyond the saturation value that is known for initially deuterium free, displacement-damaged tungsten by nearly a factor of two. Both observations together indicate that deuterium is stabilizing the defects created within the collision cascade.

Keywords: defect stabilisation, deuterium retention, self-damaged tungsten, Displacement damage, Ion radiation effects, Nuclear Reaction Analysis, temperature programmed desorption

38 **1. Introduction**

39 In order to achieve tritium self-sufficiency in a future fusion reactor, the limitation in terms of
40 tritium uptake needs to be very stringent [1]. Among many other favourable properties
41 intrinsically low fuel retention makes tungsten, therefore, one material of choice as plasma-facing
42 material. However, during plasma operation defects in the tungsten lattice will evolve that will
43 trap hydrogen isotopes. While for present day experiments this increased fuel retention is only
44 limited to the near surface it will take place throughout the whole bulk in future nuclear devices
45 as a consequence of the 14 MeV neutron irradiation. High energy ion implantation is often used
46 as a surrogate to study the effect of displacement damage on fuel retention [2,3,4,5].
47 Understanding hydrogen isotopes uptake, transport, retention and release in such displacement
48 damaged tungsten is necessary to extrapolate to reactor conditions. Experiments with fission-
49 neutron-irradiated samples as well as MeV-energy ion-implanted samples showed that hydrogen
50 isotope retention can reach values of the order of 1 at.% due to the displacement damage [4,6].
51 However, nearly all these experiments were done sequentially: First, damage was produced and
52 only then transport and retention of deuterium in this material was studied by exposing it to
53 hydrogen plasmas, ions or atom beams. In order to extrapolate to reactor conditions experiments
54 are lacking where displacement damage is created simultaneously under the presence of
55 hydrogen. Theoretical work by Kato et al. [7] as well as Middleburg [8] showed that hydrogen
56 can stabilize vacancies and lower the formation threshold for vacancy formation and hence it is
57 expected and often speculated that defect densities and as a consequence hydrogen isotope
58 retention increases for simultaneous exposures. First beam experiments where displacement
59 damage was created with MeV tungsten ion implantation while simultaneously dosing the
60 samples with atomic deuterium revealed that even the presence of very small amounts of
61 deuterium in the bulk can increase defect density and hence retention noticeably [9,10].

62 Here a different approach is presented that allows to study the influence of hydrogen isotopes
63 on damage creation: by implanting 20 MeV tungsten into already displacement-damaged and
64 deuterium containing tungsten. The idea behind it is that within the collision cascade not only
65 tungsten atoms are displaced but also trapped deuterium is de-trapped and hence displacement
66 damage takes place simultaneously under the presence of deuterium. In the first part of this
67 manuscript the experimental procedure is outlined. Afterwards calculations about the expected
68 amount of de-trapped deuterium are presented. In the following the measured total amounts of
69 deuterium and the depth distributions are presented and discussed as obtained with nuclear
70 reaction analysis (NRA) and temperature programmed desorption (TPD). Finally, rate equation
71 modelling is presented to derive the de-trapping energies and describe the observations and
72 discuss the results.

73

74 **2. Experiment**

75

76 Hot-rolled tungsten specimens were used in this study, $12 \times 15 \times 0.8 \text{ mm}^3$ in size. All
77 samples were taken from the same manufacturing batch produced by Plansee AG (Austria) with a
78 purity of 99.97 wt.%. [11]. The surfaces were mechanically polished down to 5 μm grit and
79 subsequently electro-polished in 1.5 % NaOH solution to a mirror-like finish [12]. As the aim of
80 this study was to investigate the effects of the MeV ion implantation within the ion range of about
81 2 μm samples were heat treated to reduce the intrinsic defect density and hence retention in the
82 bulk. Specimens were heated at 2000 K for 2 min by electron bombardment in vacuum at a
83 pressure below 10^{-8} Pa . Afterwards the material exhibits grains with a size distribution ranging
84 from 10 μm to 50 μm as observed by confocal microscopy [13] and the initial dislocation density
85 of $2 \times 10^{12} \text{ m/m}^3$ is reduced by two orders of magnitude compared to the as-delivered state [14].

86 Displacement damage was created by tungsten self-implantation with 20 MeV W^{6+} ions
87 at the TOF beamline of the IPP tandem accelerator laboratory at room temperature. Details of the
88 setup and the procedure can be found in [13]. The ‘quick calculation of damage’ option in the
89 Monte-Carlo-based code SRIM-2008.04 (Stopping and Range of Ions in Matter) [15] was used to
90 calculate the damage profile as well as the damage dose in the same way as described in [13]. As
91 this calculation option is based on the modified Kinchin Pease formalism a subscript ‘KP’ will be
92 used in the following when stating the calculated damage dose in displacements per atom dpa_{KP} .
93 A value for E_d of 90 eV was used as recommended by the American Society for Testing and
94 Materials [16]. For 20 MeV W the calculated damage profile shows a maximum around 1.4 μm
95 and extends up 2.3 μm as can be seen in figure 1. Deuterium retention is known to saturate at
96 large damage doses [4 and references therein] and the aim of this study was to work with samples
97 damaged to this level so that further damaging conducted later on would not increase deuterium
98 retention. As in most of the articles in literature the actual input parameters used to derive the
99 stated dpa values are missing a preceding study was conducted to measure the actual value were
100 saturation sets in for the experimental parameters used in this study. Saturation was observed
101 above 7.87×10^{17} W/m² which converts to a calculated damage dose at the peak maximum of
102 $0.23 dpa_{KP}$ [17]. For the present study this tungsten fluence was chosen. Homogeneous
103 implantation was obtained by scanning the beam over other the whole sample area. The time
104 needed to acquire the desired fluence was 50 min and hence the average damage rate was 8×10^{-5}
105 dpa/s.

106 Defects were decorated with deuterium by exposing them to a well characterized low-
107 temperature electron-cyclotron-resonance deuterium plasma [18]. To minimize the possible
108 production of additional trapping sites during deuterium loading and to decorate only the existing
109 defects plasma exposure was performed with floating target holder. At a D_2 background pressure
110 of 1.0 Pa this results in an ion energy below 15 eV. Because the ion flux consists mainly of D_3^+
111 ions (94 %) with minor contributions of D_2^+ (3 %) and D^+ (3 %) we refer to this setting as

112 <5 eV/D. For this condition the resulting D flux in the form of ions is 5.6×10^{19} D/m²s. Five
113 samples were loaded at the same time for 72 h which corresponds to a fluence of 1.5×10^{25} D/m².
114 Each sample was tightly screwed at the four corners to a tungsten coated copper target holder
115 with molybdenum screws. A sample temperature of 370 K was chosen small enough to avoid any
116 defect annealing during D loading yet large enough to allow for D diffusion into the depth. The
117 temperature was maintained by a liquid heating circuit connected to thermostats operated with
118 silicon oil at 373 K. A thermocouple pressed against the back of the target holder and an IR
119 camera was used to monitor the temperature evolution as well as the lateral homogeneity during
120 the experiments. The IR camera was calibrated directly before plasma operation using the
121 thermostat at the desired temperature. As it is essential in this study that not only the applied
122 tungsten fluence is high enough to reach the level saturation of displacement damage but also that
123 the created damage zone is completely filled one sample was decorated for a second time for
124 another 72 h. The deuterium depth profiles for that sample is shown in figure 1 (2nd decoration)
125 together with the one for a sample that saw deuterium plasma only once (1st decoration). In both
126 cases deuterium has diffused down to two micrometer depth and the maximum concentration is
127 1.7 at-%. The difference in the depth profiles are marginal. Hence, one can conclude that the
128 damage zone for all samples is completely filled after 72 h.

129 Deuterium depth profiles were analysed ex-situ with the $D(^3\text{He},p)\alpha$ nuclear reaction with
130 eight different ³He energies ranging from 500 keV to 4.5 MeV to probe a sample depth of up to
131 7.4 μm . The D concentration within the near-surface layer at depths of up to about 0.3 μm was
132 determined with ³He energies of 500 keV, 690 keV and 800 KeV by analyzing the emitted α
133 particles with a surface barrier detector at the laboratory scattering angle of 102°. A rectangular
134 slit in front of the detector reduces the solid angle to 9.16 msr but increases resolution. For
135 determining the D concentration at larger depths, the high energy protons were analyzed using a
136 thick, large angle PIPS (Passivated Implanted Planar Silicon) detector at a scattering angle of

137 135°. A nominal pre-set charge of 10 μC was accumulated for each energy. Backscattered ^3He
 138 particles were detected with another PIPS detector positioned at 165° in Cornell geometry to

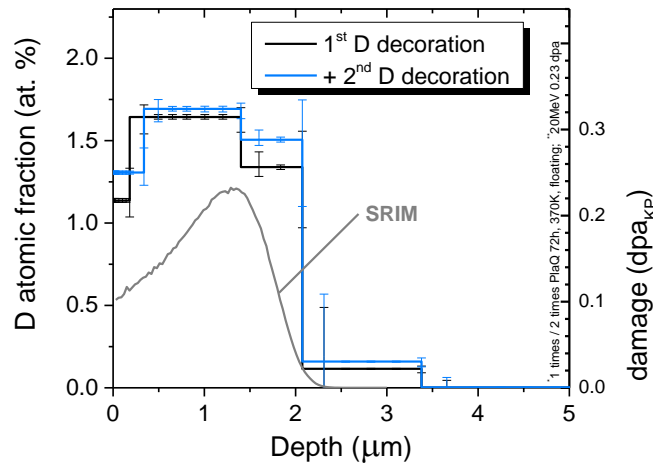


Figure 1: Deuterium depth profiles for two self-damaged tungsten samples decorated once (1st D decoration) and twice (+ 2nd D decoration) with 1.5×10^{25} D/m². The calculated damage profile for the applied W fluence of 1.87×10^{17} W/m² is shown in addition (grey line, right scale).

139

140 determine the actual accumulated charge for each individual energy. SIMNRA 6.06 was used to
 141 simulate the RBS spectra with SRIM stopping powers [15]. Details of the setup can be found in
 142 [13] and [19]. NRADC [20] and SIMNRA [21] were used to deconvolute the NRA spectra
 143 measured at different ^3He ion energies. As input data for NRADC all α and proton spectra
 144 measured at the different energies were analyzed simultaneously. Details about the data
 145 evaluation using NRADC can be found in Ref. [21]. The cross section published by Wielunska et
 146 al. [22] and Besenbacher and Möller [23] were used. The total amount of D retention was finally
 147 determined by integrating the D profile over the measured depth. To check the performance of the
 148 detectors and to minimize the scatter in absolute D areal densities in our measurements a gold
 149 coated, amorphous, deuterated carbon thin film calibration sample (*a*-C:D) of known D content

150 was measured for each energy in addition. The accuracy of the beam current measurement
151 (typically 3-5 %) together with the counting statistics of about 1 % (counts depending on D
152 content and energy) assures that the reproducibility of our measurements stays within 5 %. The
153 absolute accuracy is dominated by the accuracy of the cross section which is stated as 5 %, too
154 [23]. After the NRA measurement the retained D amount of the specimens was measured by
155 temperature programmed desorption (TPD) in the quartz tube of the TESS device. A basic
156 description of TESS is given in [24]. The temperature response of the samples to the linear oven
157 temperature ramp was calibrated in independent experiments by a thermocouple spot-welded to a
158 tungsten sample of identical size and surface finish. The samples were heated up to a sample
159 temperature of 1010 K with an oven heating ramp of 3 K/min. This maximum temperature of
160 1010 K is high enough to ensure desorption of all retained D from the samples. The desorbed
161 gases were measured with a quadrupole mass spectrometer (Pfeiffer/Inficon DMM 422). The
162 secondary electron multiplier of the QMS was operated in single ion counting mode to minimize
163 the background noise and to be able to apply Poisson statistics for determining the accuracy.
164 Selected masses between 2 and 44 amu/q were recorded as a function of time (so called multiple
165 ion detection mode of the QMS). The following 15 masses were recorded: 1, 2, 3, 4, 12, 14, 16,
166 17, 18, 19, 20, 28, 32, 40, and 44 amu/q. Release was dominated by mass channel 4 and 1. Mass
167 channels above 4 showed no significant release of deuterium containing species other than HD
168 and D₂. Background contributions were determined in a preceding and a consecutive temperature
169 ramp without a sample or an outgassed sample in the heating zone, respectively. Measurements
170 showed only negligible contributions in mass channel 4 and contributions on the percentage range
171 for mass channel 3 which was subtracted in the latter case. For the quantitative analysis the QMS
172 signal for D₂ was calibrated after each temperature ramp with a Laco leak bottle with a flow of
173 2.48×10^{19} D₂/s and a stated accuracy of 4.6 %. The calibration factor for HD was experimentally
174 determined by flowing D₂ and HD gas through an orifice of know size from a calibrated volume.
175 Based on the pressure recording of a spinning rotor gauge the calibration factor in QMS counts

176 per molecule for HD was 66 % of the one derived for D₂. Contribution of HD on the total D
177 desorption was less than 2.4%. The reproducibility of the total signal heights of 3 % was derived
178 by consecutive calibration measurements and is governed by the stability of the detector. The
179 accuracy for the absolute amount for D is hence determined by the stated accuracy of the leak
180 valve for the measurement shown here.

181
182

183 **2. Results and discussion**

184

185 *3.1 Calculating deuterium de-trapping*

186

187 The Monte-Carlo-based code SDTrimSP 5.07 (Static-Dynamic TRansport of Ions in Matter
188 Sequential and Parallel processing) [25] was used to simulate the depth distribution of deuterium
189 recoils generated during the implantation of tungsten into the deuterium containing tungsten.
190 SDTrim.SP is typically used to describe physical sputtering of target atoms from the near surface.
191 Recently Ziegler-Biersack stopping powers were implemented to be able to describe also
192 displacement damage in the same way as SRIM [15] does. The dominant parameter in this case is
193 the energy E_{dis} that is necessary to displace a tungsten atom from its lattice site and produce a
194 stable Frenkel pair. In order to derive a value for the number of deuterium atoms that get
195 displaced an adequate energy has to be chosen. Typical thermal de-trapping energies of deuterium
196 from defects in tungsten as derived from rate equation modelling range between 0.8 eV and 2 eV
197 [26].

198 Here we assume that the kinetic energy a tungsten atom has to transfer to a deuterium atom in
199 order to de-trap it from its defect site is the same as this thermal de-trapping energy. For
200 simplicity an average value of 1 eV was assumed for the calculation. Figure 2 shows the depth
201 profile of the number of de-trapped deuterium atoms normalized to the initially retained
202 deuterium for a tungsten sample containing 2 at-% of deuterium for the given tungsten fluence of

203 $7.87 \times 10^{17} \text{ W}^{6+}/\text{m}^2$ and energy of 20 MeV. One can see that the fraction of de-trapped deuterium
 204 atoms varies by a factor of two between the surface and the peak maximum located around
 205 1.5 μm . In the damage peak maximum on average every D atoms is replaced once during the
 206 50 minutes tungsten implantation. Hence, one would expect that mobile deuterium should be

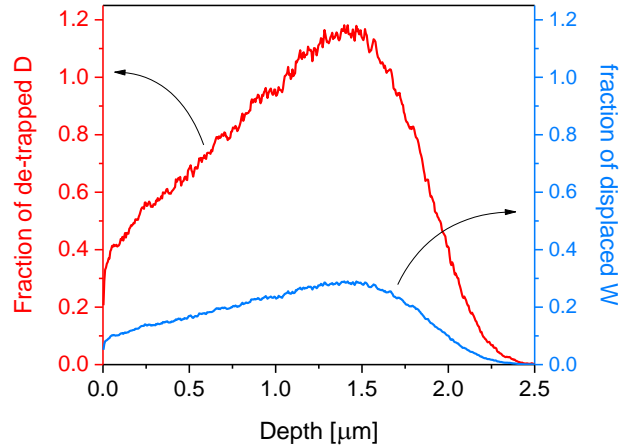


Figure 2: Dynamic SDTrimSP calculation of the number of de-trapped deuterium atoms normalized to the initially retained deuterium atomic fraction of 2% and the number of displaced W atoms normalized to the W bulk density as function of depth. Tungsten implantation fluence and energy are $7.87 \times 10^{17} \text{ W}^{6+}/\text{m}^2$ and 20 MeV, respectively. Deuterium de-trapping and W displacement energies are 1.0 eV and 90 eV, respectively.

207
 208 present simultaneously while the tungsten atoms are displaced. The number of calculated
 209 displaced tungsten atoms is also shown (right scale). However, care must be taken when
 210 comparing the number of displaced tungsten atoms with the number of de-trapped deuterium
 211 atoms. In the present case a displacement energy of 90 eV was used for tungsten as recommended
 212 by the American Society for Testing and Materials in order to compare with existing neutron
 213 irradiation results [16]. However, it is known that actual displacement energies are substantially
 214 lower and depend on crystal orientation [27]. If a value of 40 eV would have been used the

215 calculated displacement damage would be a factor of 2.2 higher. Hence, the ratio between de-
216 trapped deuterium atoms per displaced tungsten atoms would not be four but only two. Given the
217 uncertainties about the actual displacement energies in both calculations all what we want to
218 conclude here is that the number of de-trapped deuterium atoms and displaced tungsten atoms is
219 within the same order of magnitude.

220

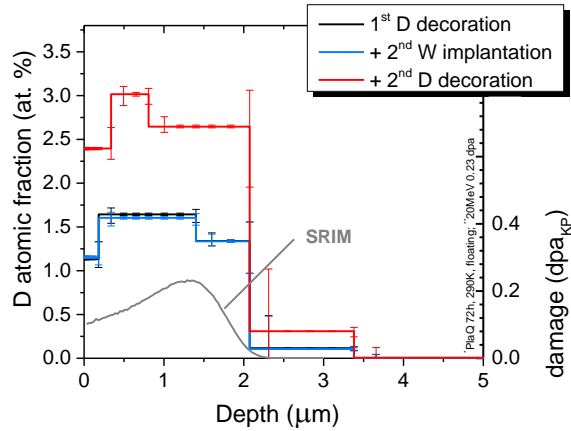
221 *3.2 W implantation into self-damaged, D-containing tungsten*

222

223 Figure 3a shows again the deuterium depth profile from figure 1 for a sample implanted with
224 20 MeV tungsten to a fluence of 7.87×10^{17} W/m² and then decorated with deuterium for 72 h
225 afterwards (1st D decoration, black line). In addition, the depth profile for a sample implanted
226 with 20 MeV tungsten to a fluence of 7.87×10^{17} W/m² for another time is shown (+ 2nd W
227 implantation, blue line). Both samples show the identical flat depth profile, ranging down to
228 2 μ m. No deuterium is lost, neither to the surface, nor to the bulk. While the latter is expected as
229 there is no creation of traps in the bulk where deuterium could be retained one could have
230 expected that some deuterium is lost to the surface. Obviously re-trapping of the deuterium that is
231 released by the tungsten bombardment is very effective. Figure 3b shows the corresponding
232 deuterium effusion fluxes of these two samples as function of time during the heating ramp in the
233 same colors together with the sample temperature (green line, right axis). For the sample
234 decorated once desorption of deuterium starts around 345 K and ends at around 980K. It shows
235 two distinct maxima, one at 560 K and one at 780 K. While the depth profile for the sample
236 implanted additionally with tungsten did not show any difference to the initial one, the deuterium
237 desorption is substantially altered by the tungsten implantation: The first desorption peak is
238 significantly depleted while the second one is increased. Significant deuterium desorption does
239 not start before 500 K and the peak maximum is shifted to 635 K. The position of the second

240 desorption maximum is not altered as well as the maximum temperature up to which desorption
 241 takes place is also unchanged.

a)



b)

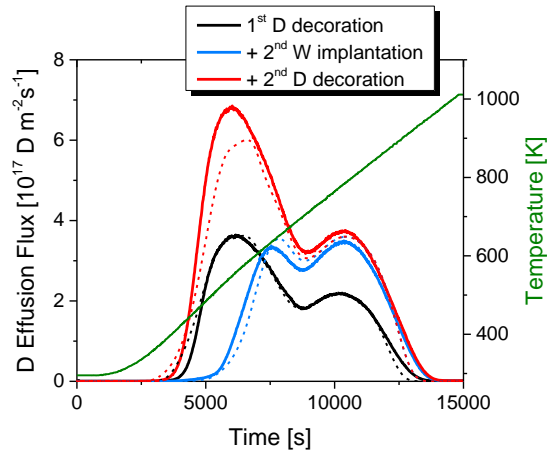


Figure 3: Deuterium depth profiles (a) and deuterium effusion flux as function of time (b) for self-damaged tungsten samples decorated once (1st D decoration, black line) and implanted again with 20 MeV tungsten to a fluence of 1.87×10^{17} W/m² (+2nd W implantation, blue line). In red, the data for a sample decorated with deuterium for 72 h again after the second W implantation is shown. In (a) the calculated W displacement damage is plotted in addition (grey line, right scale) and in (b) the sample temperature (right scale) and the results from the rate equation modelling are shown (dashed lines).

242

243

3.3 Reloading of self-damaged, D containing tungsten

244

245

246

247

248

249

250

251

252

253

254

255

256

257

258

259

In order to find out if additional trapping sites were created during the tungsten implantation of the deuterium containing, self-damaged tungsten one sample was exposed again to the low-temperature deuterium plasma. Exposure conditions were the same as for the initial defect decoration with floating target, exposed for 72 h at a temperature of 370 K. As shown before, no change in the deuterium depth profile was observed when only doubling the D fluence as for the given energy, flux and temperature no additional defects are observed. However for this sample that saw the additional W implantation there is a dramatic change in the depth profile as well as the desorption spectrum: While the overall shape of both stayed the same, the absolute intensities nearly doubled. The depth profile for this sample shows now a peak concentration of 3 at.%. The desorption spectrum indicates that the tungsten implantation did not create defects with substantially different de-trapping energies but it seems that only the total densities of defects were increased. This is at first glance surprising as the sample that also saw the additional W implantation but no additional D decoration afterwards did show a substantially altered desorption spectrum. Therefore rate equation modelling was conducted to describe the observed phenomena.

260

261

3.4 Rate equation modelling

262

263

264

265

266

267

268

269

270

271

272

273

274

The rate equation code TESSIM-X was used to describe the observed phenomena [28,29]. TESSIM-X can simulate the transport and interaction of different hydrogen isotopes in tungsten based on the physical model of de-trapping, diffusion and trapping. Two different physical models can be used: The first is the so-called classical model which is characterized by the assumption that each trap can be occupied by only one hydrogen atom and each trap type has a fixed de-trapping energy. The second option is the so-called fill-level model, inspired by DFT calculations [30 and references therein], which assumes that each trap can be filled with several hydrogen atoms simultaneously. Here the latter was used because the de-trapping energies necessary to describe thermal desorption were taken from an independent study where deuterium-hydrogen isotope exchange in self-damaged tungsten could be described quantitatively [31]. One trap with five fill levels with de-trapping energies of 1.18, 1.32, 1.46, 1.7, 1.84 eV, and a pre-factor of 10^{13} Hz were found to describe the thermal effusion spectra. The diffusion coefficient

275 for protium $D_0 = 1.58 \times 10^{-7} \text{ m}^2/\text{s}$ was divided by $\sqrt{2}$ to account for the higher mass of deuterium
276 and a migration energy of 0.25 eV was used [32]. The trap profile were derived from the
277 measured deuterium depth profiles and a trap density of 0.32 at. %, which corresponds
278 approximately to one fifth of the measured D concentration, is chosen. The following sequence
279 was modelled with TESSIM-X: First, a 100 μm thick tungsten slab with a 2.2 μm thick top layer
280 was filled with D with the given flux and fluence. The deuterium flux distribution was taken from
281 [18]. It was assumed that D_2^+ and D_3^+ ions can be described as D^+ ions with twice or three times
282 the flux but only half or one third of the energy, respectively. The corresponding D implantation
283 profile was approximated by truncated Gaussians fits to implantation profiles calculated with
284 SDTrimSP. After the given D fluence the sample was cooled to room temperature and after a
285 waiting time of 2000 s the temperature of the sample was ramped up according to the measured
286 temperature. Figure 3b shows the obtained calculated deuterium desorption spectrum as a dashed
287 black line. The description of the desorption is excellent. The peak positions as well as their width
288 and height are very well reproduced. In order to describe the desorption spectrum of the sample
289 that was additionally implanted with tungsten correctly, two effects had to be considered. First
290 the creation of additional traps due to the displacement damage caused by 20 MeV W^{6+} ions and
291 second the kinetic de-trapping of trapped D by collisions with energetic atoms in the tungsten ion
292 collision cascade.

293 The effect of additional traps was approximated by increasing the trap density while leaving the
294 de-trapping energies as well as the depth distribution of the traps unchanged.

295 The trap density was assumed to increase in the same way with irradiated tungsten fluence as
296 observed in a preceding study with deuterium-free tungsten where it saturated at a fluence of
297 $7.87 \times 10^{17} \text{ W}^{6+}/\text{m}^2$ [17]. Based on these data the additional W self-damaging was simulated by an
298 exponentially saturating increase of the trap density up to 1.8 times of the original trap density
299 during the W implantation.

300

301 The kinetic de-trapping of trapped D by energetic W was investigated with SDTrimSP in which
302 the implantation of 20 MeV W into D containing W was simulated. The D concentration was
303 varied between 1 to 5 at. % and the displacement energy of D was altered within the range of the
304 de-trapping energies of the fill-levels from 0.5 to 2.0 eV. For each SDTrimSP simulation the
305 depth profile of the D recoils was extracted and normalized by the respective D concentration.
306 The so obtained kinetic de-trapping profiles of D by W were fitted by an asymmetric Gaussian
307 which allows the parameterization of the profiles with respect to the individual de-trapping
308 energies of the fill-levels used in the TESSIM-X simulation. After the initial loading of the

309 sample with D and the subsequent waiting time of 2000 s the W self-damaging is simulated with
310 a W flux of 2.62×10^{14} 1/m²s for 3000 s at a temperature of 300 K. During this period the trap
311 density was increased and the kinetic de-trapping of trapped D took place as described above.
312 Once the W implantation was finished an additional waiting time of 2000 s was simulated before
313 the temperature was increased. It can be seen in figure 3b that the simulation reproduces the
314 measured desorption spectrum very well. The depletion of the first desorption peak as well as the
315 increase of the second one are in good agreement with the experimental observation. It is
316 important to stress that the shift in the release temperature is due to the increased trap density and
317 not due to a different de-trapping-energy as would be typically concluded in the literature.
318 The D reloading of the additionally self-damaged, D-containing tungsten sample was simulated as
319 above but with an additional D loading sequence following the additional W implantation phase
320 after a waiting time of 2000 s. Once the second D loading was finished and 2000 s of waiting
321 time passed, the temperature of the sample was ramped up. The simulated desorption spectrum is
322 compared to the experimental data in figure 3b. Also in this case the agreement between
323 simulation and experiment is very good. Especially the increase of the first desorption peak while
324 the second one remains nearly unchanged is reproduced by the simulation.

325
326

327 Figure 4 shows the calculated deuterium solute concentration as a function of depth for
328 different times during the 20 MeV tungsten implantation into the self-damaged tungsten
329 containing 1.7 at.% D. Similarly as the W damage profile the solute concentration extends to
330 2.3 μm and shows a maximum at a depth of 1.4 μm . At the very beginning of the tungsten
331 implantation the solute concentration builds up quickly and reaches a value of 5×10^{-8} at.%. It is
332 worth mentioning that this solute concentration is within the same order of magnitude as
333 calculated for the existing experiments with two beams [9,10]. Therefore it is important to note
334 that the effect of de-trapping of retained deuterium within the collision cascade needs to be taken
335 into account also when modelling such multi beam exposures when the amount of deuterium
336 builds up over time. For the present experiment the solute concentration drops for two reasons as
337 implantation continues. First, the number of newly created traps increases and with increasing
338 amount of traps the solute concentration drops. Second, the average fill level drops and hence the
339 effective de-trapping energy increases with evolving time.

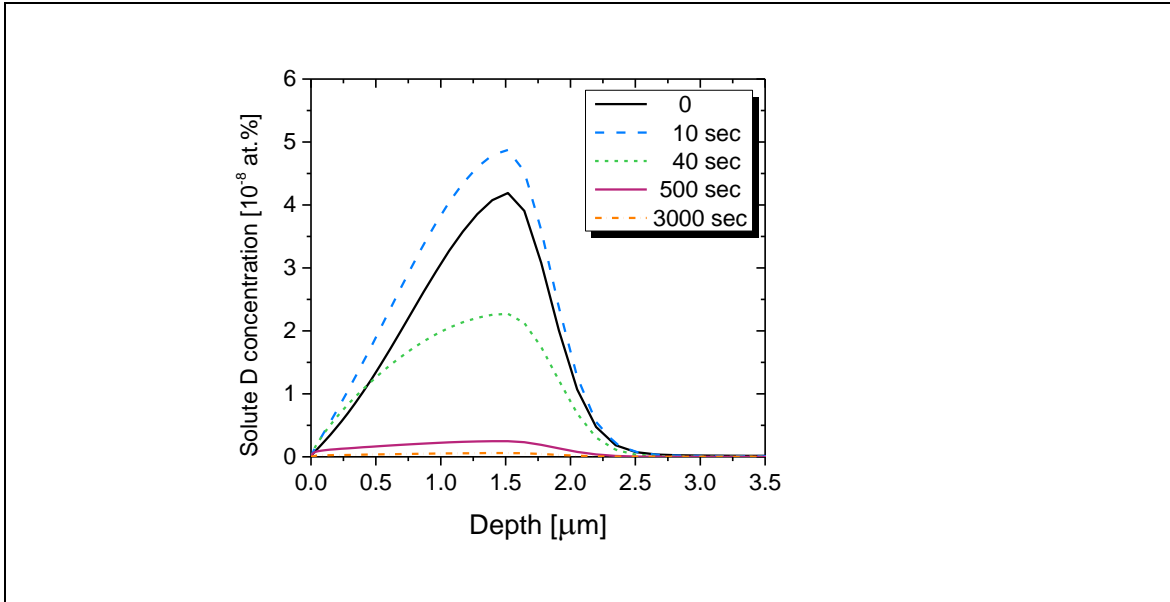


Figure 4: Calculated deuterium solute concentration as a function of depth for different times during the 20 MeV tungsten implantation into the self-damaged tungsten containing 1.7 at.% D.

340

341 In summary, both experiments can be explained by an increase in trap densities. The
 342 maximum deuterium concentration is nearly a factor of two higher as ever observed for self-
 343 damaged but initially deuterium-free tungsten. This clearly indicates that deuterium can stabilize
 344 defects. At present experiments are under way to study the effect of damage stabilization as a
 345 function of the initially retained deuterium amount. Next, it will be investigated up to which
 346 temperature this increased retention prevails.

347

348

349 4. Conclusions

350

351 An alternative experimental approach to study the influence of deuterium on displacement
 352 damage in tungsten is presented: In contrast to evolved dual beam experiments where damage is
 353 created within the displacement cascade of MeV energy ions while dosing the sample with
 354 deuterium atoms [9] or low energy ions [33] at the same time here only one beam is necessary.
 355 Deuterium containing self-damaged tungsten is used as starting material and bombarded with
 356 MeV energy ions. Due to the de-trapping of the retained deuterium from the traps within the
 357 collision cascade deuterium gets re-trapped and hence the newly created displacement damage
 358 also takes place simultaneously with mobile deuterium being present. Monte-Carlo based
 359 simulations of the collision process show that for the parameters used on average every retained
 360 deuterium atom is de-trapped once. Experiments reveal that no deuterium is lost from the self-

361 damaged tungsten sample when it is bombarded with 20 MeV tungsten again. However,
362 deuterium is de-trapped and effectively re-trapped again. Temperature programmed desorption
363 spectroscopy shows that deuterium is redistributed from the low temperature de-trapping peak to
364 the high temperature de-trapping peak. Rate equation modelling can describe the change in
365 deuterium desorption by assuming only an increase in trap density without changing the de-
366 trapping energies compared to the initial material. Decorating the samples after the second
367 tungsten implantation again with a low-energy deuterium plasma bolsters this assumption as
368 deuterium retention increases beyond the value that is known for initially deuterium free,
369 displacement-damaged tungsten by nearly a factor of two. Both experimental observations show
370 that deuterium is stabilizing the defects created within the collision cascade. As a consequence
371 this substantially increased retention must be considered when extrapolating to reactor conditions
372 based on sequential experiments where displacement damage was created before deuterium
373 exposure. The same effect of increased retention is not only expected for laboratory experiments
374 but also for reactor operation where displacement damage in tungsten will take place in the bulk of
375 the material by fusion neutrons while deuterium and tritium will be present in the material from
376 the plasma implantation.

377

378 **Acknowledgments**

379

380 The authors thank T. Dürbeck, J. Dorner and M. Fusseder, for their technical support. This work
381 has been carried out within the framework of the EUROfusion Consortium and has received
382 funding from the Euratom research and training programme 2014–2018 under grant agreement
383 No. 633053. Work was performed under EUROfusion WP PFC. The views and opinions
384 expressed herein do not necessarily reflect those of the European Commission.

385

386

-
- [1] G.R. Tynan, R.P. Doerner, J. Barton, R. Chen, S. Cui, M. Simmonds, Y. Wang, J.S. Weaver, N. Mara, and S. Pathak. “Deuterium Retention and Thermal Conductivity in Ion-Beam Displacement-Damaged Tungsten.” *Nuclear Materials and Energy*, June 2017. <https://doi.org/10.1016/j.nme.2017.03.024>.
- [2] W.R. Wampler, and R.P. Doerner. “The Influence of Displacement Damage on Deuterium Retention in Tungsten Exposed to Plasma.” *Nuclear Fusion* 49, no. 11 (November 2009): 115023. <https://doi.org/10.1088/0029-5515/49/11/115023>.
- [3] B. Tyburska, V.Kh. Alimov, O.V. Ogorodnikova, K. Schmid, and K. Ertl. “Deuterium Retention in Self-Damaged Tungsten.” *Journal of Nuclear Materials* 395, no. 1–3 (December 2009): 150–55. <https://doi.org/10.1016/j.jnucmat.2009.10.046>. et al. *J. Nucl. Mater.* 395 (2009)
- [4] V.Kh. Alimov, Y. Hatano, B. Tyburska-Püschel, K. Sugiyama, I. Takagi, Y. Furuta, J. Dörner, et al. “Deuterium Retention in Tungsten Damaged with W Ions to Various Damage Levels.” *Journal of Nuclear Materials* 441, no. 1–3 (October 2013): 280–85. <https://doi.org/10.1016/j.jnucmat.2013.06.005>.
- [5] S. Markelj, O.V. Ogorodnikova, P. Pelicon, T. Schwarz-Selinger, K. Sugiyama, and I. Čadež. “Study of Thermal Hydrogen Atom Interaction with Undamaged and Self-Damaged Tungsten.” *Journal of Nuclear Materials, Proceedings of the 20th International Conference on Plasma-Surface Interactions in Controlled Fusion Devices*, 438, Supplement (July 2013): S1027–31. <https://doi.org/10.1016/j.jnucmat.2013.01.224>.
- [6] M. Shimada, G. Cao, T. Otsuka, M. Hara, M. Kobayashi, Y. Oya, and Y. Hatano. “Irradiation Effect on Deuterium Behaviour in Low-Dose HFIR Neutron-Irradiated Tungsten.” *Nuclear Fusion* 55, no. 1 (January 1, 2015): 013008. <https://doi.org/10.1088/0029-5515/55/1/013008>.
- [7] D. Kato, H. Iwakiri, Y. Watanabe, K. Morishita, and T. Muroga. “Super-Saturated Hydrogen Effects on Radiation Damages in Tungsten under the High-Flux Divertor Plasma Irradiation.” *Nuclear Fusion* 55, no. 8 (August 1, 2015): 083019. <https://doi.org/10.1088/0029-5515/55/8/083019>.
- [8] S.C. Middleburgh, R.E. Voskoboinikov, M.C. Guenette, and D.P. Riley. “Hydrogen Induced Vacancy Formation in Tungsten.” *Journal of Nuclear Materials* 448, no. 1–3 (May 2014): 270–75. <https://doi.org/10.1016/j.jnucmat.2014.02.014>.
- [9] S. Markelj, T. Schwarz-Selinger, A. Založnik, M. Kelemen, P. Vavpetič, P. Pelicon, E. Hodille, and C. Grisolia. “Deuterium Retention in Tungsten Simultaneously Damaged by High Energy W Ions and Loaded by D Atoms.” *Nuclear Materials and Energy*, November 2016. <https://doi.org/10.1016/j.nme.2016.11.010>.
- [10] E. A. Hodille, S. Markelj, T. Schwarz-Selinger, A. Založnik, M. Pečovnik, M. Kelemen, C. Grisolia, „Stabilization of defects by the presence of hydrogen in tungsten: simultaneous W ion damaging and D atom exposure“, submitted to *Nuclear Fusion* (2018):
- [11] PLANSEE High Performance Materials, Reutte, Austria.
- [12] A. Manhard , G. Matern , M. Balden , A step-by-step analysis of the polishing process for tungsten specimens, *Pract. Metallogr.* 50 (1) (2013) 6–15.
- [13] T. Schwarz-Selinger, “Deuterium Retention in MeV Self-Implanted Tungsten: Influence of Damaging Dose Rate.” *Nuclear Materials and Energy*, March 2017. <https://doi.org/10.1016/j.nme.2017.02.003>.

-
- [14] A. Manhard, M. Balden, S. Elgeti, Quantitative microstructure and defect density analysis of polycrystalline tungsten reference samples after different heat treatments, *Pract. Metallorg.* 52 (2015) 437.
- [15] J.F. Ziegler, www.srim.org.
- [16] ASTM Int'l E521-96 Standard Practice for Neutron Radiation Damage Simulation by Charge-Particle Irradiation, Annual Book of ASTM Standards vol 12.02 (Philadelphia, PA: American Society for Testing and Materials) p 7 DOI
- [17] T. Schwarz-Selinger, S. Markelj, J. Bauer, A. Manhard, K. Schmid, in preparation.
- [18] A. Manhard, T. Schwarz-Selinger, W. Jacob, *Plasma Sources Sci. Technol.* 20 (2011) 015010.
Note: Unfortunately, the information given in the last paragraph of this article is not correct. The contribution of the molecular ions to the total ion flux for standard conditions is: $D_3^+ = 94\%$, $D_2^+ = 3\%$, and $D^+ = 3\%$. Correspondingly, the contributions to the total deuteron flux in form of ions are: 97%, 2%, and 1% as expressed correctly in figures 5 and 6 in this reference.
- [19] Wielunska, B., M. Mayer, and T. Schwarz-Selinger. "Optimization of the Depth Resolution for Deuterium Depth Profiling up to Large Depths." *Nuclear Instruments and Methods in Physics Research Section B: Beam Interactions with Materials and Atoms* 387 (November 15, 2016): 103–14. <https://doi.org/10.1016/j.nimb.2016.09.004>.
- [20] K. Schmid and U. von Toussaint, *Nucl. Instr. and Meth. in Phys. Res. B* 281 64 (2012).
- [21] M. Mayer, SIMNRA User's Guide, Report IPP 9/113, Max-Planck-Institut für Plasmaphysik, Garching, Germany, 1997 and <http://www.rzg.mpg.de/~mam/>.
- [22] B. Wielunska, M. Mayer, T. Schwarz-Selinger, U. von Toussaint, and J. Bauer. "Cross Section Data for the $D(^3\text{He},p)^4\text{He}$ Nuclear Reaction from 0.25 to 6MeV." *Nuclear Instruments and Methods in Physics Research Section B: Beam Interactions with Materials and Atoms*, October 2015. <https://doi.org/10.1016/j.nimb.2015.09.049>.
- [23] W. Möller and F. Besenbacher. "A Note on the $^3\text{He}^+ \text{D}$ Nuclear-Reaction Cross Section." *Nuclear Instruments and Methods* 168, no. 1–3 (January 15, 1980): 111–14. [https://doi.org/10.1016/0029-554X\(80\)91239-2](https://doi.org/10.1016/0029-554X(80)91239-2).
- [24] E. Salançon, T. Dürbeck, T. Schwarz-Selinger, F. Genoese, W. Jacob, *J. Nucl. Mater.* 376 (2008) 160.
- [25] A. Mutzke, R. Schneider, W. Eckstein, and R. Dohmen, "SDTrimSP version 5.00 IPP 12/8," Max-Planck-Institut für Plasmaphysik, Garching, Germany, 2011. [Online]. Available: http://pubman.mpdl.mpg.de/pubman/item/escidoc:2139848:1/component/escidoc:2139847/IP_P%2012_8.pdf
- [26] E.A. Hodille, A. Založnik, S. Markelj, T. Schwarz-Selinger, C.S. Becquart, R. Bisson, and C. Grisolia. "Simulations of Atomic Deuterium Exposure in Self-Damaged Tungsten." *Nuclear Fusion* 57, no. 5 (May 1, 2017): 056002. <https://doi.org/10.1088/1741-4326/aa5aa5>.
- [27] A. De Backer, A. Sand, C.J. Ortiz, C. Domain, P. Olsson, E. Berthod, and C.S. Becquart. "Primary Damage in Tungsten Using the Binary Collision Approximation, Molecular Dynamic Simulations and the Density Functional Theory." *Physica Scripta T167* (February 20, 2016): 014018. <https://doi.org/10.1088/0031-8949/T167/1/014018>.
- [28] K. Schmid, U. von Toussaint, and T. Schwarz-Selinger. "Transport of Hydrogen in Metals with Occupancy Dependent Trap Energies." *Journal of Applied Physics* 116, no. 13 (October 7, 2014): 134901. <https://doi.org/10.1063/1.4896580>.
- [29] K. Schmid, J. Bauer, T. Schwarz-Selinger, S. Markelj, U. von Toussaint, A. Manhard, and W. Jacob. "Recent Progress in the Understanding of H Transport and Trapping in W." *Physica Scripta T170* (December 1, 2017): 014037. <https://doi.org/10.1088/1402-4896/aa8de0>.
- [30] N. Fernandez, Y. Ferro, and D. Kato. "Hydrogen Diffusion and Vacancies Formation in Tungsten: Density Functional Theory Calculations and Statistical Models." *Acta Materialia* 94 (August 2015): 307–18. <https://doi.org/10.1016/j.actamat.2015.04.052>.

-
- [31] T. Schwarz-Selinger, J. Bauer, K. Schmid, and S. Markelj, in preparation.
- [32] K. Heinola, and T. Ahlgren. “First-Principles Study of H on the Reconstructed W(100) Surface.” *Physical Review B* 81, no. 7 (February 24, 2010).
<https://doi.org/10.1103/PhysRevB.81.073409>.
- [33] S. Markelj, T. Schwarz-Selinger, M. Pečovnik, A. Založnik, M. Kelemen, P. Vavpetič, P. Pelicon, in preparation.